COMPDYN 2013
4th ECCOMAS Thematic Conference on
Computational Methods in Structural Dynamics and Earthquake Engineering
M. Papadrakakis, V. Papadopoulos, V. Plevris (eds.)
Kos Island, Greece, 12–14 June 2013

DISCONTINUOUS GALERKIN METHODS FOR HIGH-DIMENSIONAL FOKKER-PLANCK EQUATIONS IN STOCHASTIC DYNAMICS

Friederike Loerke[1] **and Udo Nackenhorst**[2]

[1]Institute of Mechanics and Computational Mechanics
Appelstr. 9A, 30167 Hannover, Germany
e-mail: friederike.loerke@ibnm.uni-hannover.de

[2] Institute of Mechanics and Computational Mechanics
Appelstr. 9A, 30167 Hannover, Germany
e-mail: nackenhorst@ibnm.uni-hannover.de

Keywords: Fokker-Planck Equation, Discontinuous Galerkin Method

Abstract. *In this contribution, Discontinuous Galerkin methods are investgated as solution techniques for the high-dimensional Fokker-Planck equation (FPE). Time-Discontinuous Galerkin (TDG) methods are identified to provide stable solutions for smooth, as well as non-smooth functions. The TDG method allows for large time steps and are thus very efficient, at least for moderate dimensions. In higher dimensions, they become infeasible due to implicit coupling of the whole domain. For handling high-dimensional problems, spatial Discontinuous Galerkin (DG) methods are suggested, for their allowance of an element-wise split of the domain, and thus parallelization. The implementation of the Discontinuous Galerkin method for arbitrary dimensions is demonstrated.*

1 INTRODUCTION

The Fokker-Planck equation is a very attractive instrument for the analysis of stochastic dynamical systems under white noise excitation. It is of vast interest due to directly providing a probability density function for the system response. This is subject to the acceptance of the Markov process property for the stochastic process under consideration. The Fokker-Planck equation has its origin in the stochastic description of Brownian motion. A thorough discussion on the origin, theory and possible solution techniques is provided by RISKEN in [12]. Beyond this, the solution of the Fokker-Plank equation remains an ambitious task. Analytical solutions can only be provided for very limited special cases. Hence, investigations concentrate on numerical solution techniques. In an early study, [13], a Galerkin type approach, based on polynomial expansions, is used to solve high-dimensional stationary FPEs. A similar approach is presented in [8] for an engineering application. Despite their capability with respect to the treatment of high dimensions, these methods are often restricted regarding the shape of the approximated function. For seeking more general solutions and temporal evolution of the probability density function, Computational Fluid Dynamics solution techniques for advection-diffusion equations are suitable. Just a few contributions within this context are referred to in the following: Finite Element methods are used e.g. by [17], where domain decomposition for higher dimensions is suggested and shown for 2D and 3D. A comparison between Finite Element and Finite Difference methods can be found in [5] using the example of up to 4D non-linear oscillators. To approach the solution of higher dimensional problems, multi-scale Finite Element methods are suggested e.g. in [9], with the presentation of a two-dimensional example, and in [10] with the application to a three dimensional problem.

Within this contribution, alternative numerically stable and efficient solution techniques for the Fokker-Planck equation are investigated. Firstly, a short introduction on the derivation of the FPE is given in section 2. Afterwards, numerical solution techniques are evaluated in section 3: Diverging from traditional semi-discretization techniques, with Finite Element discretization in space and Finite Difference discretization in time, attention is drawn to the Time-Discontinuous Galerkin method. It can be shown, that the TDG method is an efficient technique for the solution of advection-diffusion equations. Nevertheless, in high dimensions the solution becomes impractical. Accordingly, a possibility to overcome this is examined, which is the spatial Discontinuous Galerkin method. Computational tests are presented, as well as the implementation for higher dimensions. Finally, an outlook on further research interests is given.

2 FOKKER-PLANCK REPRESENTATION OF STOCHASTIC DYNAMICAL PROBLEMS

In this section, a brief derivation of the Fokker-Planck equation for an examplary stochastic partial differential equation is outlined. The basis is formed by a stochastic equation of motion of a mass m, with spring constant k and damping constant d,

$$m\ddot{\mathbf{x}}(\theta,t) + d\dot{\mathbf{x}}(\theta,t) + k\mathbf{x}(\theta,t) = \mathbf{f}(\theta,t), \tag{1}$$

subject to random excitation $\mathbf{f}(\theta,t)$. θ denotes a random variable. The system stochastics are restricted by the following assumption: The uncertain excitation is regarded as Gaussian white noise, see [15], which is perfectly characterized by its first and second moments, see[16]. In particular, the ensemble average is $\langle f(t)\rangle = 0$ and the process is delta-correlated for two different instants of time, t and t', meaning that $\langle f(t)f(t')\rangle = \delta(t-t')$, which is further explained in [12]. This implicates that the system response also forms a Markov vector process, meaning

that every state only depends on the known present state, and is fully independent of previous states. With this property, the response statistics of the system can be computed from the transition probability density function. Therefore, they result from the Fokker-Planck equation, which characterizes the temporal evolution of the probability density function. To illustrate this, the probability density of the motion is described as follows

$$p(\mathbf{x},t) = \langle \prod_{i=1}^{n} \delta(x_i - x_i(t)) \rangle, \tag{2}$$

with the $2n$-dimensional vector $\mathbf{x} = [x_1 \ \dot{x}_1 \ \dots \ x_n \ \dot{x}_n]^\mathsf{T}$, consisting of coordinates x_i and velocities $\dot{x}_i$. Equation (2) is transformed into the transport equation

$$\frac{\partial}{\partial t} p(\mathbf{x},t) = -\sum_{i=1}^{n} \frac{\partial}{\partial x_i} \langle \prod_{i=1}^{n} \delta(x_i - x_i(t)) \frac{\partial x_i}{\partial t} \rangle. \tag{3}$$

This reduces to the advection-diffusion-type Fokker-Planck equation:

$$\frac{\partial}{\partial t} p(\mathbf{x},t) = \frac{\partial}{\partial x_i} \left(\mathbf{c}(\mathbf{x},t) p(\mathbf{x},t) \right) + \frac{\partial}{\partial x_i \partial x_j} \left(\mathbf{D}(\mathbf{x},t) p(\mathbf{x},t) \right), \tag{4}$$

wherein the first term is an advection term with the advection velocity vector $\mathbf{c}$ and the second term is the diffusion term with the coefficient $\mathbf{D}$.

3 NUMERICAL SOLUTION

The numerical solution of advection-diffusion equations remains a challenging task, due to the opposed characteristics of advection and diffusion terms. Standard techniques like Finite Difference methods and Finite Volume methods face the difficulty that the advection term is better resolved within explicit time stepping schemes and the diffusion is only efficiently and correctly resolved within implicit time integration, [14]. Otherwise, grave numerical errors due to oscillation would be introduced by the advection term, most notably for non-smooth functions. While explicit treatment of the diffusion term would imply the necessity of very small time steps. Often, the inconvenience of oscillations, induced by the advection term, is coped with the introduction of artificial diffusion, like within the Streamline Upwind/Petrov-Galerkin method (see e.g. [1]). In this work, the introduction of artificial terms is sought to avoid. An efficient solution technique to meet the demands of both advection and diffusion terms turns out to be the Time-Discontinuous Galerkin method, which is discussed in the following subsection. In the subsequent part, attention is drawn to the implementation in higher dimensions. Therefore, the TDG method has to be dropped in favour of a spatial Discontinuous Galerkin method.

3.1 Time-Discontinuous Galerkin Method

Spatial discretization can be either achieved by Finite Volumes or Finite Differences, as well as Finite Elements. Here, the latter is chosen to allow for local high order resolution. Instead of Finite Differences or Runge-Kutta methods, in this work, the time domain is also resolved with Finite Elements, leading to a full Galerkin scheme in space and time. Additionally, element-wise decoupling is allowed in the time domain, to avoid errors induced by oscillations. Those types of schemes are referred to as Discontinuous Galerkin methods. They were proposed amongst others by REED and HILL in [11] with first analyses to be found in [6] and [4]. A

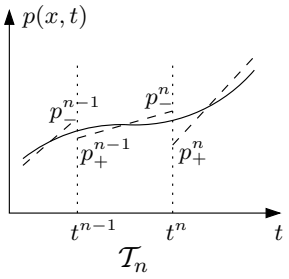

Figure 1: discontinuous shape functions in time

discussion on the TDG method for pure advection is provided in [18].
In particular, the TDG method is conducted as follows: First, the partial differential equation (4) is transformed into a weak form coupled in time and space, by multiplication with a weighting function η and integration over the time and spatial domains $\mathcal{T}_n$ and $\mathcal{B}$:

$$\eta \int_{\mathcal{T}_n} \int_{\mathcal{B}} \frac{\partial p}{\partial t} + \nabla \cdot (\mathbf{c}p - \mathbf{D}\nabla p)\,\mathrm{d}\Omega\,\mathrm{d}t = 0. \tag{5}$$

The dependencies on $\mathbf{x}$ and t are omitted for brevity.
The probability density and the weighting function are approximated by finite element shape functions in space and time, while discontinuities are assumed at the boundaries of each time interval,

$$p_+^n = \lim_{s\to 0}\, p(t^n + s),\; p_-^n = \lim_{s\to 0}\, p(t^n - s) \Rightarrow \text{ jump: } [|p^n|] = p_+^n - p_-^n, \tag{6}$$

as depicted in figure (1). The discrete form of equation (5) for an element Ω_e reads

$$\begin{aligned} &\underbrace{\left[\int_{\mathcal{T}_n} \tilde{N}^T \tilde{N}_{,t}\,\mathrm{d}t + \tilde{N}_+^T(t^{n-1})\tilde{N}_+(t^{n-1})\right]}_{\boldsymbol{\Upsilon}_a} \int_{\Omega_e} \eta_h p_h\,\mathrm{d}\Omega \\ &+ \underbrace{\left[\int_{\mathcal{T}_n} \tilde{N}^T \tilde{N}\,\mathrm{d}t\right]}_{\boldsymbol{\Upsilon}_b} \int_{\Omega_e} \left(-\frac{\partial D_i}{\partial x_i}\eta_h p_h - D_i \eta_h \frac{\partial p_h}{\partial x_i} + D_{ij}\frac{\partial \eta_h}{\partial x_i}\frac{\partial p_h}{\partial x_j} + \frac{\partial \eta_h}{\partial x_i} p_h \frac{\partial D_{ij}}{\partial x_j}\right)\mathrm{d}\Omega \\ &= \underbrace{\left[\tilde{N}_+^T(t^{n-1})\tilde{N}_-(t^{n-1})\right]}_{\boldsymbol{\Upsilon}_c} \int_{\Omega_e} \eta_h p_h^{n-1}\,\mathrm{d}\Omega, \end{aligned} \tag{7}$$

with the temporal shape functions $\tilde{N}$, their time derivatives $\tilde{N}_{,t}$, the discrete test functions η_h and discrete solution p_h, as well as the time matrices $\boldsymbol{\Upsilon}_i$. Inserting continuous shape functions in space $\mathbf{H}$, a non-symmetric linear system of equations is obtained:

$$\underbrace{[\boldsymbol{\Upsilon}_a(t) \otimes \mathbf{M} + \boldsymbol{\Upsilon}_b(t) \otimes \mathbf{Q}]}_{\hat{\mathbf{K}}}[\hat{\mathbf{p}}] = [\boldsymbol{\Upsilon}_c(t) \otimes \mathbf{M}\hat{\mathbf{p}}^{n-1}], \tag{8}$$

with the mass matrix

$$\mathbf{M} = \int_{\Omega_e} \mathbf{H}^T \mathbf{H}\,\mathrm{d}\Omega \tag{9}$$

and the advection and diffusion matrix

$$\mathbf{Q} = \int_{\Omega_e} \Bigg(\underbrace{-\frac{\partial D_i}{\partial x_i}\mathbf{H}^T\mathbf{H} - D_i\mathbf{H}^T\mathbf{H}_{,x_i}}_{\text{advection}} + \underbrace{D_{ij}\mathbf{H}^T_{,x_i}\mathbf{H}_{,x_j} + \mathbf{H}^T_{,x_i}\mathbf{H}\frac{\partial D_{ij}}{\partial x_j}}_{\text{diffusion}} \Bigg) \mathrm{d}\Omega. \tag{10}$$

The TDG scheme enables the use of large time steps and, thus, Courant numbers $Cr = c_i\frac{\Delta t}{\Delta x_i} \gg 1$. Increasing the order of time integration TDG(i) allows for a huge increase in time step size, without negative effects on stability.

To demonstrate the solution of the Fokker-Planck equation, the response of a random white noise excited Van-der-Pol oscillator is computed. The equation of motion for the 1D Van-der-Pol oscillator with system parameters α and β under white noise excitation $\omega(t)$ reads

$$\ddot{x} - (\alpha - \beta x^2)\dot{x} + x = \omega(t). \tag{11}$$

This equation is transformed into the Fokker-Planck equation

$$\frac{\partial p}{\partial t} = -\frac{\partial p}{\partial x} + \frac{\partial}{\partial \dot{x}}\left[\beta x^2\dot{x} - \alpha\dot{x} + x\right] + D\frac{\partial^2 p}{\partial \dot{x}^2} \tag{12}$$

which is solved with the TDG method. In figure (2) the result of the computation is shown, which is a solution on a limit cycle in the phase space, as expected. The Fokker-Planck equation for the one-dimensional oscillator with two degrees of freedom, position and velocity, is a two-dimensional equation, requiring two-dimensional Finite Elements for the solution scheme plus time discretization. Thus, it is easily comprehensible that a system with higher degrees of freedom would lead to a higher *dimensional* Fokker-Planck equation, i.e. a two-mass oscillator with four degrees of freedom, two positions and two velocities, would lead to a four-dimensional Fokker-Planck equation. This is still computable on a desktop computer, but looking on the system matrix growth scheme, the limit of continuous FEM is clearly visible:

matrix size $= (TDG(i)+1)((nel+1)np-nel+1)^n.$

$TDG(i)$: order of TDG
nel: number of elements/dimension
np: order of spatial approx.
n: dimension

Herein, the *curse of dimensionality* comes out very obviously, because the dimension is incorporated in the exponent. To overcome this curse, a split of the spatial domain seems promising, which entails the idea of a Discontinuous Galerkin method in space.

3.2 Spatial Discontinuous Galerkin Method

The spatial Discontinuous Galerkin method for the Fokker-Planck equation is defined according to the representations by COCKBURN and SHU for the classical advection-diffusion equation, see for instance [2]. Initially, the Fokker-Planck equation is rewritten in a compact form,

$$\frac{\partial p(\mathbf{x},t)}{\partial t} + \underbrace{\nabla\cdot(\mathbf{c}p(\mathbf{x},t)}_{\nabla\cdot\mathbf{f}(p(\mathbf{x},t),\mathbf{x},t)} - \mathbf{D}\nabla p(\mathbf{x},t)) = 0, \tag{13}$$

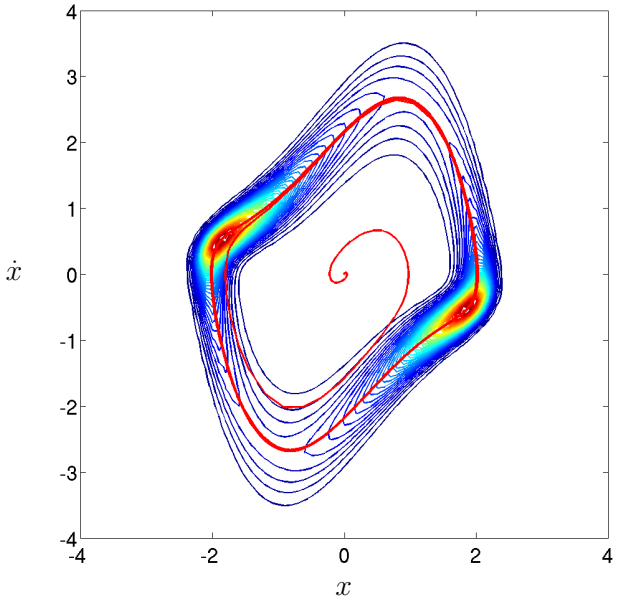

Figure 2: contour plot of the probability density distribution of a white noise excited Van-der-Pol oscillator on the limit cylce (red line)

wherein an advection flux $\mathbf{f}$ and a diffusion flux $\mathbf{D}\nabla p$ can be identified. Again omitting the dependence on $\mathbf{x}$ and t and inserting a variable $\boldsymbol{\sigma} = \bar{\mathbf{D}}\nabla p$, with $\mathbf{D} = \bar{\mathbf{D}}^2$, leads to the system of equations,

$$\frac{\partial p}{\partial t} + \nabla \cdot \mathbf{f}(p) - \nabla \cdot \left(\bar{\mathbf{D}}\boldsymbol{\sigma}\right) = 0 \quad \text{and} \quad \boldsymbol{\sigma} - \bar{\mathbf{D}}\nabla p = 0, \tag{14}$$

analoguous to the formulation in [2]. The coupled weak form after multiplications with the weighting functions η and ζ and integration over the domain reads

$$\begin{aligned} &\frac{\partial}{\partial t}\int_{\mathcal{B}} p\eta \,\mathrm{d}\Omega + \int_{\mathcal{B}} \left[\nabla \cdot \mathbf{f}(p) - \nabla \cdot \left(\bar{\mathbf{D}}\boldsymbol{\sigma}\right)\right] \eta \,\mathrm{d}\Omega \quad = 0 \\ &\text{and} \qquad \int_{\mathcal{B}} \boldsymbol{\sigma}\zeta \,\mathrm{d}\Omega - \int_{\mathcal{B}} \nabla \cdot \mathbf{d}\zeta \,\mathrm{d}\Omega = 0, \end{aligned} \tag{15}$$

with $\mathbf{d} = \bar{\mathbf{D}}p$. Integration by parts of each second term in equations (15) leads to the boundary terms,

$$\int_{\partial\mathcal{B}} \eta \left[\mathbf{f} - \mathbf{D}\boldsymbol{\sigma}\right] \cdot \mathbf{n} \,\mathrm{d}\Gamma \qquad \text{and} \qquad \int_{\partial\mathcal{B}} \zeta \mathbf{d} \cdot \mathbf{n} \,\mathrm{d}\Gamma, \tag{16}$$

including the normal vector $\mathbf{n}$. The boundary terms are non-unique under the precondition of allowing discontinuities at the inter-element boundaries. Consequently, the terms have to be substituted by numerical flux terms, so that the coupled local discretized weak form reads:

$$\begin{aligned} &\int_{\mathcal{B}_e} \mathbf{H}^T\mathbf{H} \,\mathrm{d}\Omega_e \,\hat{\mathbf{p}}_{,t} + \sum_{f\in\partial\mathcal{B}_e} \int_{\mathcal{B}_f} \mathbf{H}_f^T \left(\mathbf{f}^* - (\bar{\mathbf{D}}\boldsymbol{\sigma})^*\right) \,\mathrm{d}\Omega_f - \int_{\mathcal{B}_e} \mathbf{H}_{,x}^T \left[\mathbf{f}(p_h) - \bar{\mathbf{D}}(p_h)\boldsymbol{\sigma}\right] \,\mathrm{d}\Omega_e = 0 \\ &\text{and} \qquad \int_{\mathcal{B}_e} \mathbf{H}^T\mathbf{H} \,\mathrm{d}\Omega_e \hat{\boldsymbol{\sigma}} - \sum_{f\in\partial\mathcal{B}_e} \int_{\mathcal{B}_f} \mathbf{H}_f^T \mathbf{d}^* \,\mathrm{d}\Omega_f + \int_{\mathcal{B}_e} \mathbf{H}_{,x}^T \mathbf{d}(p_h(t,x)) \,\mathrm{d}\Omega_e = 0, \end{aligned} \tag{17}$$

wherein the index e denotes the element domain and f denotes the element face domain. For the numerical flux terms, denoted by an asterisk, any consistent flux can be chosen. COCKBURN and SHU suggest the so-called Local Discontinuous Galerkin (LDG) fluxes in [3]. This is the Lax-Friedrichs flux (see, e.g. [7]) for the advective part,

$$\mathbf{f}^*(p^-, p^+) == \frac{1}{2}\left[\mathbf{f}(p_h^-)\cdot\mathbf{n}_{f,\partial\mathcal{B}_e} + \mathbf{f}(p_h^+)\cdot\mathbf{n}_{f,\partial\mathcal{B}_e} - \alpha_{f,\partial\mathcal{B}_e}(p_h^+ - p_h^-)\right], \tag{18}$$

with the inside element solution value p^- and the outside element solution value p^+, as well as the local maximum flux velocity $\alpha_{f,\partial\mathcal{B}_e}$. The discrete numerical diffusion flux is chosen as

$$\begin{aligned}(\bar{\mathbf{D}}\sigma)^* &= \sum_{i=1}^{dim}\frac{(d_{i,h}^+ - d_{i,h}^-)}{(p_h^+ - p_h^-)}\frac{1}{2}\left[\sigma_{i,h}^-\cdot\mathbf{n}_{f,\partial\mathcal{B}_e} + \sigma_{i,h}^+\cdot\mathbf{n}_{f,\partial\mathcal{B}_e}\right]\\ &\quad + C_{11}(p_h^+ - p_h^-) + \sum_{i=1}^{dim} C_{1i}(\sigma_{i,h}^+ - \sigma_{i,h}^-) \text{ and}\\ \mathbf{d}^* &= \frac{1}{2}\left[d_{i,h}^-\cdot\mathbf{n}_{f,\partial\mathcal{B}_e} + d_{i,h}^+\cdot\mathbf{n}_{f,\partial\mathcal{B}_e}\right] - C_{1i}(p_h^+ - p_h^-).\end{aligned} \tag{19}$$

Details on the LDG flux terms can be found in [3].
This brings about a fully local system of equations, so that element-wise decoupling in explicit schemes is applicable without lumping the mass matrices. Here, the significant advantage of the spatial Discontinuous Galerkin method emerges: The problem of working memory deficit can be overcome through element-wise decoupling and even parallel treatment of the possibly high-dimensional system.

Examples

The Discontinuous Galerkin method allows for steep gradients in the approximated function, if the polynomial order of the local shape functions is increased. In figure (3(a)), the decrease of oscillations within the advection of a non-smooth function, computed with DG methods of increasing order is depicted to demonstrate the stability of the method. The quantity $p0$ is the initial condition, p_ref is the analytical reference solution and p the numerically computed solution for the chosen time step.
A second DG-test, shown in figure (3(b)), is the two-dimensional Molenkamp test. This is again a test for pure advection, as the main challenge within the Fokker-Planck equation is the correct resolution of the advection term.

n-Dimensional Discretization

Another challenge is the treatment of high dimensions. Therefore, an arbitrary high-dimensional Finite Element mesher has been implemented for regular meshes. Node coordinates and element incidences can be easily obtained by dimension-dependent permutations, which end up in meshes as depicted in figure (4), for a 4D example. In this example, the domain is discretized with three elements per coordinate direction, meaning that four nodal positions exist per direction. Two exemplary elements (15 and 68) are plotted. Node and element numbering are arranged depending on the dimension, from negative to positive coordinate direction, starting from direction $\mathbf{e}_1$. In this manner, mesh generation is carried out for any number of

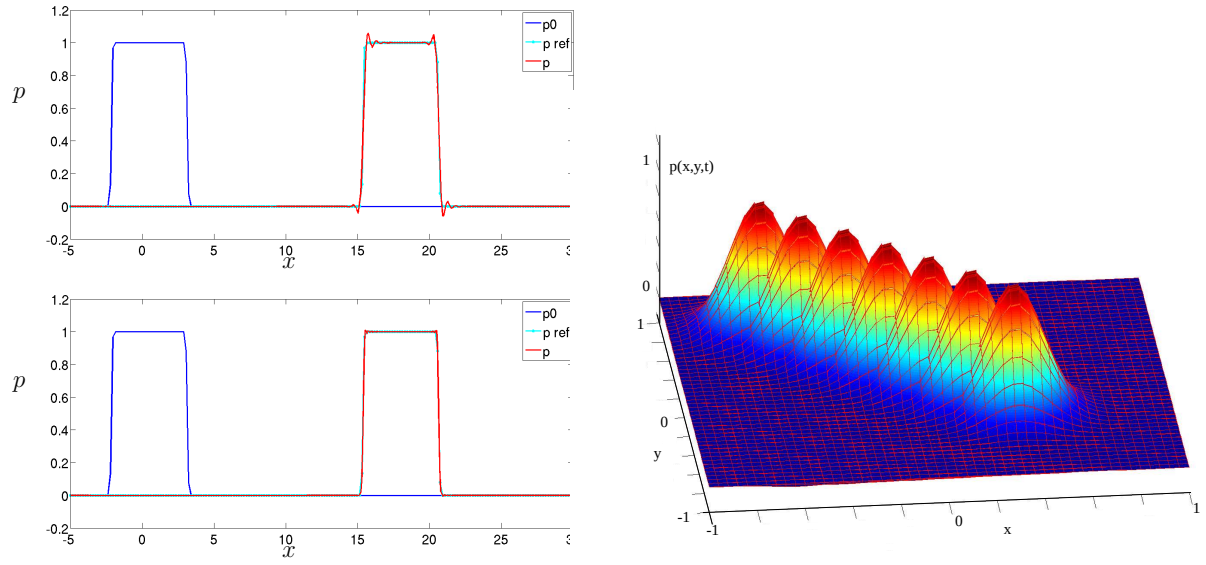

(a) 1D DG(3) and DG(7) with steep gradients (b) 2D Molenkamp test

Figure 3: resolution of pure advection with Discontinuous Galerkin methods

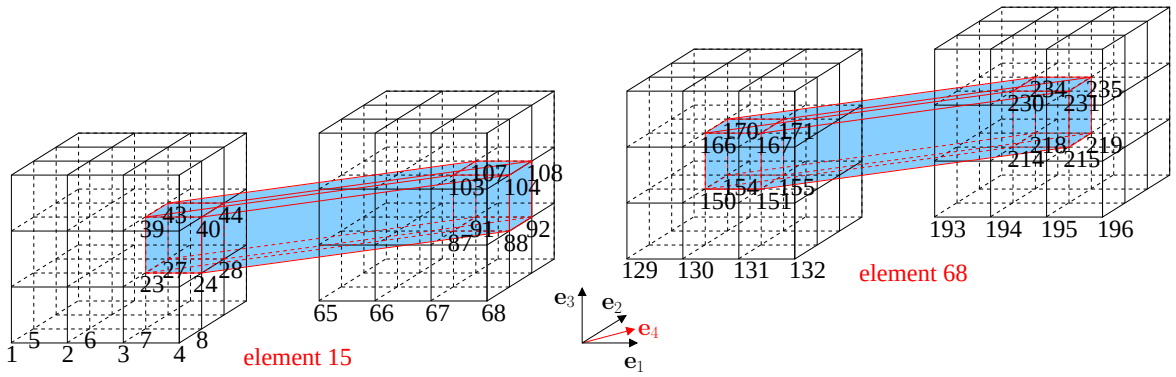

Figure 4: 4-dimensional mesh, 3 elements per dimension, exemplary depiction of element 15 and 68

dimensions n. To support this statement, the generation of n-dimensional unit elements is depicted in figure (5) An n-dimensional element can always be built up through a projection of the $n-1$-dimensional element.

For arbitrary dimensional unit elements, shape functions of polynomial order np can be computed as the n-fold product of the np-order Lagrangian polynomials.

After having defined mesh data and shape functions for n-dimensional problems, it remains to compute the n-dimensional flux vector over all 2^n faces of dimension $n-1$. Therefore, $n-1$-dimensional shape functions are needed, as well as the n-dimensional normal vector in global coordinates. This vector can be computed through orthogonalization of a vector with respect to the row vectors of the surface Jacobian.

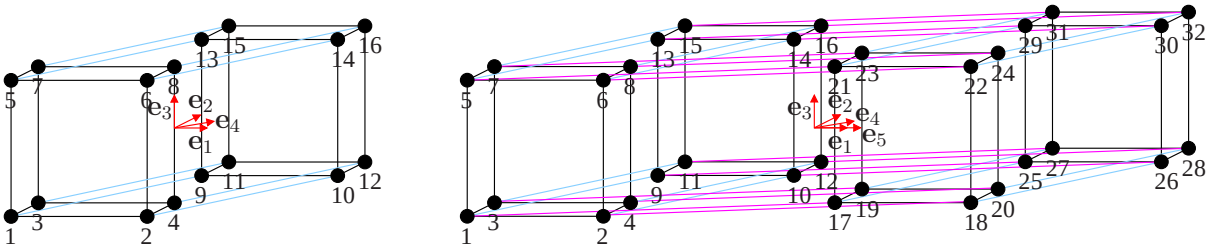

(a) 4D element (b) 5D element

Figure 5: unit elements

4 OUTLOOK

The Discontinuous Galerkin method is a promising and applicable technique for the solution of high-dimensional Fokker-Planck equations. It allows for element-wise parallelization, as the system of equations is completely locally decoupled. Adaptive mesh refinement is very suitable for the method, as a result of the allowance of discontinuities at inter-element boundaries. Furthermore, two neighbouring elements can be discretized in completely different scales.
The LDG resolution of the diffusion part with local explicit time integration, is not the perfect choice, due to the time step restriction. In the future, implicit-explicit schemes should be implemented as a replacement.

REFERENCES

[1] Alexander N. Brooks and Thomas J.R. Hughes. Streamline Upwind/Petrov-Galerkin formulations for convection dominated flows with particular emphasis on the incompressible Navier-Stokes equations. *Comput. Meth. Appl. Mech. Eng.*, 32:199–259, 1982.

[2] B. Cockburn and C.W. Shu. Runge-Kutta discontinuous Galerkin methods for convection-dominated Problems. *Journal of Scientific Computing*, 16(3):173–261, 2001.

[3] Bernardo Cockburn and Chi-Wang Shu. The local discontinuous Galerkin method for time-dependent convection-diffusion systems. *SIAM J. Numer. Anal.*, 35:2440–2463, 1998.

[4] C. Johnson and J. Pitkäranta. An analysis of the discontinuous Galerkin method for a scalar hyperbolic equations. *Math. Comput.*, 46(173):1–26, 1986.

[5] Pankaj Kumar and S Narayanan. Solution of Fokker-Planck equation by finite element and finite difference methods for nonlinear systems. *Sadhana-Acad. P. Eng. S.*, 31:445–461, 2006.

[6] P. Lesaint and P.A. Raviart. On a finite element method for solving the neutron transport equation. *Mathematical Aspects of Finite Elements in Partial Differential Equations*, pages 89–122, 1974.

[7] R.J. LeVeque. *Finite Volume Methods for Hyperbolic Problems*. Cambridge Texts in Applied Mathematics. Cambridge University Press, 2002.

[8] Wolfram Martens, Utz von Wagner, and Volker Mehrmann. Calculation of high-dimensional probability density functions of stochastically excited nonlinear mechanical systems. *Nonlinear Dynamics*, 67:2089–2099, 2012.

[9] Arif Masud and Lawrence A. Bergmann. Application of multi-scale finite element methods to the solution of the Fokker-Planck equation. *Computer Methods in Applied Mechanics and Engineering*, 194:1513 – 1526, 2005.

[10] L. Pichler, A. Masud, and L.A. Bergman. Numerical solution of the Fokker-Planck equation by Finite Difference and Finite Element Methods - A comparative study. In Manolis Papadrakakis, George Stefanou, and Vissarion Papadopoulos, editors, *Computational Methods in Stochastic Dynamics*, volume 26 of *Computational Methods in Applied Sciences*, pages 69–85. Springer Netherlands, 2013.

[11] W.H. Reed and T.R. Hill. Triangular mesh methods for the neutron transport equation. *Los Alamos Report LA-UR-73-479*, 1973.

[12] Hannes Risken. *The Fokker-Planck Equation Methods of Solution and Applications*. Springer-Verlag Berlin, 1996.

[13] C. Soize. Steady-state solution of Fokker-Planck equation in higher dimension. *Probabilistic Engineering Mechanics*, 3:196 – 206, 1988.

[14] Gilbert Strang. *Computational science and engineering*. Wellesley-Cambridge Press Wellesley, MA, 2007.

[15] R. L. Stratonovich and Richard A. Silverman. *Topics in the Theory of Random Noise*, volume 1. Gordon and Breach New York, 1963.

[16] N. G. Van Kampen. *Stochastic processes in physics and chemistry*, volume 1. North-Holland, 1981.

[17] W. Yi, B.F. Spencer Jr, and L.A. Bergman. Solution of the Fokker-Planck equation in higher dimensions: application of the concurrent finite element method. In *Shiraishi N, Shinozuka M, Wen YK. 7th International Conference on Structural Safety and Reliability (ICOSSAR97), November*, 1997.

[18] Matthias Ziefle and Udo Nackenhorst. Numerical techniques for rolling rubber wheels: treatment of inelastic material properties and frictional contact. *Comput. Mech.*, 42:337–356, 2008.